Aerosol Science and Technology

ISSN: 0278-6826 (Print) 1521-7388 (Online) Journal homepage: www.tandfonline.com/journals/uast20

Evaluation of a catalytically aided thermal regeneration method for quartz filter-based black carbon sensing

Xiaochen Tang, Minrui Wei, Fred Brechtel & Thomas W. Kirchstetter

To cite this article: Xiaochen Tang, Minrui Wei, Fred Brechtel & Thomas W. Kirchstetter (2026) Evaluation of a catalytically aided thermal regeneration method for quartz filter-based black carbon sensing, Aerosol Science and Technology, 60:9, 1016-1024, DOI: 10.1080/02786826.2026.2659051

To link to this article: https://doi.org/10.1080/02786826.2026.2659051

© 2026 Lawrence Berkeley National Labrotary. Published with license by Taylor & Francis Group, LLC

View supplementary material

Published online: 13 May 2026.

Submit your article to this journal

Article views: 278

View related articles

View Crossmark data

Full Terms & Conditions of access and use can be found at
https://www.tandfonline.com/action/journalInformation?journalCode=uast20

AEROSOL SCIENCE AND TECHNOLOGY
2026, VOL. 60, NO. 9, 1016–1024
https://doi.org/10.1080/02786826.2026.2659051

OPEN ACCESS Check for updates

Evaluation of a catalytically aided thermal regeneration method for quartz filter-based black carbon sensing

Xiaochen Tang[a], Minrui Wei[b], Fred Brechtel[c], and Thomas W. Kirchstetter[a,b]

[a]Energy Technologies Area, Lawrence Berkeley National Laboratory, Berkeley, California, USA; [b]Civil and Environmental Engineering Department, University of California, Berkeley, California, USA; [c]Brechtel Manufacturing Inc, Hayward, California, USA

ABSTRACT

Black carbon (BC)–a strong indicator of diesel particulate matter and other sources of incomplete carbonaceous fuel combustion–is an important air pollutant that affects public health, yet low-cost sensors capable of long-term, autonomous BC monitoring remain underdeveloped. We report on the development and evaluation of a novel BC prototype sensor that integrates soot collection on a quartz filter, in-situ optical transmission measurement, and thermal filter regeneration. To enable regeneration at lower temperatures, we evaluated the catalytic effects of various alkali metal salts pre-applied to the filter. Among these, cesium carbonate (Cs_2CO_3) exhibited the strongest catalytic activity, lowering the temperature required for complete BC removal by up to 190 °C and reducing energy consumption by more than 75% compared to that required for untreated filters. The catalytic effect persisted through 10 BC collection–regeneration cycles. These findings demonstrate the potential of catalytically aided thermal regeneration in BC sensors and suggest a pathway toward energy-efficient and reduced maintenance air quality monitoring suitable for distributed BC monitoring networks.

GRAPHICAL ABSTRACT

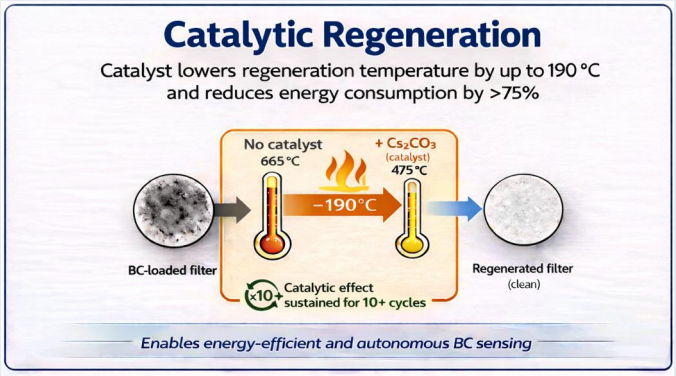

ARTICLE HISTORY
Received 9 October 2025
Accepted 17 March 2026

EDITOR
Akua Asa-Awuku

1. Introduction

The widespread adoption of low-cost air pollution sensors reflects their value to researchers and public agencies for dense monitoring networks and the public's growing interest in understanding air quality inside and outside their homes and workplaces (Kumar et al. 2015; Lewis et al. 2016; Morawska et al. 2018; Karagulian et al. 2019; Liu et al. 2020). The most affordable and user-friendly sensors, which employ laser particle counters to estimate fine

CONTACT Xiaochen Tang xtang@lbl.gov Energy Technologies Area, Lawrence Berkeley National Laboratory, Berkeley, CA 94720.
Supplemental data for this article can be accessed online at https://doi.org/10.1080/02786826.2026.2659051.
Editor: Akua Asa-Awuku

© 2026 Lawrence Berkeley National Labrotary. Published with license by Taylor & Francis Group, LLC
This is an Open Access article distributed under the terms of the Creative Commons Attribution-NonCommercial-NoDerivatives License (http://creativecommons.org/licenses/by-nc-nd/4.0/), which permits non-commercial re-use, distribution, and reproduction in any medium, provided the original work is properly cited, and is not altered, transformed, or built upon in any way. The terms on which this article has been published allow the posting of the Accepted Manuscript in a repository by the author(s) or with their consent.

particulate matter ($PM_{2.5}$) concentrations and transmit data in real time, have achieved the widest adoption (Stavroulas et al. 2020; Heintzelman et al. 2023; Lassalle 2024). Some low-cost PM sensors (such as Clarity node-s air sensor n.d. and Airvisual pro indoor monitor n.d.) also measure gaseous species, including carbon dioxide (CO_2), nitrogen dioxide (NO_2), and volatile organic compounds (VOCs).

$PM_{2.5}$ is an important air pollutant linked to adverse health effects. It originates from various primary sources and is also formed through atmospheric reactions. Measuring specific components of $PM_{2.5}$ is valuable, for example, in communities with heightened exposure to diesel particulate matter, such as those near seaports, freeways, and other freight hubs where diesel trucks, locomotives, and vessels operate. In prior work, Caubel et al. (2018) developed a black carbon (BC) sensor—a strong indicator of diesel particulate matter—for community-engaged air monitoring, and deployed 100 units for 100 days in West Oakland, California (Caubel et al. 2019). These sensors have since been used in other communities (e.g., Sugrue et al. 2024), reflecting growing interest in hyperlocal BC measurements to better assess exposure to diesel emissions. However, such deployments have typically been limited to a few weeks due to the need for frequent manual filter replacement, which increases both operational complexity and cost. While BC analyzers equipped with self-advancing filter tape reels (e.g., aethalometers) are commercially available, their high cost has hindered widespread adoption in communities, unlike the more cost-effective sensors previously referenced.

This manuscript describes initial steps toward developing a BC sensor capable of autonomous thermal filter regeneration, which could significantly extend periods of unattended deployment. Specifically, results are presented for a prototype sensor that collects soot on a quartz filter, thermally regenerates the filter, and optically measures soot collection and removal. We also systematically investigated metal salts as catalysts to lower the combustion temperature of BC, assessing their stability over multiple thermal regeneration cycles. Additionally, we evaluated the energy requirements for regeneration using different filter heater geometries. Reducing the combustion temperature is critical for practical applications, as it lowers thermal and oxidative stress on sensor components and reduces energy consumption, thereby extending operational life and minimizing storage needs. This is an especially important benefit for off-grid or remote locations. These improvements ultimately decrease maintenance frequency and overall cost.

Several studies have established the catalytic potential of alkali metal salts for BC combustion (Mochida and Miyazaki 1998; Jiménez et al. 2008; Legutko et al. 2023). Kirchstetter and Novakov (2007) demonstrated that co-collecting sodium chloride (NaCl) with BC aerosols on quartz filters reduced the BC combustion temperature by approximately 150 °C compared to BC alone. Similarly, Neeft et al. (1998) examined the oxidation rates of carbon black catalyzed by various alkali metal carbonates, finding that cesium carbonate (Cs_2CO_3) had a stronger catalytic effect than potassium carbonate (K_2CO_3) and sodium carbonate (Na_2CO_3). Importantly, these salts maintain their catalytic activity over repeated thermal cycles (Peng et al. 2008; Skrbek et al. 2022), making them attractive for applications requiring repeated regeneration. A renewed interest in this catalytic behavior has been spurred by the needs of modern low-cost air quality sensing. The push for dense, distributed monitoring networks requires sensors that are energy-efficient and capable of long-term, autonomous operation (Caubel et al. 2018). In this study, we leverage this catalytic chemistry to enable the repeated thermal regeneration necessary for practical, portable black carbon monitors.

The catalyst operates *via* an oxygen-transfer (redox) cycle, where the alkali metal salt acts as an oxygen carrier between the gas phase and the carbon surface (McKee 1983; Suzuki et al. 1992). First, the carbon reduces the alkali metal salt to form an intermediate. This intermediate is then re-oxidized by atmospheric oxygen, regenerating the catalyst. This process creates reactive oxygen species such as alkali oxides and peroxides that migrate to the catalyst interface. These species lower the activation energy required to break C-C bonds, accelerating the conversion of carbon into CO and CO_2 (McKee 1983; Kapteijn et al. 1986; Neeft et al. 1998). Cesium-based catalysts are especially effective in this role due to the high mobility of the cesium cation at elevated temperatures, which maintains a stable, active interface with the solid soot and promotes oxidation at temperatures far below the typical thermal threshold (Chen and Yang 1992; Neeft et al. 1998). This study evaluates the catalytic combustion performance of various alkali metal salts on both laboratory flame-generated BC particles and ambient atmospheric aerosols.

2. Methods

2.1. Laboratory flame-generated BC collection

An inverted methane-air diffusion flame (Kirchstetter and Novakov 2007) was used to generate BC that was

collected on quartz fiber filters (Pallflex 2500 QAT-UP). Briefly, incomplete combustion of methane and air produces a controllable and high concentration of BC particles, whose sizes are in the range of those generated by modern engines, with insignificant amounts of organic carbon (Stipe et al. 2005). A portion of the diluted effluent from the combustion was drawn through quartz filters in stainless steel filter holders and in the prototype sensor described below. The flame apparatus is a prolific BC source, enabling rapid sample collection at 1–2 L min^{-1} and 5–7 min per sample.

2.2. Ambient aerosol collection

Our laboratory features an anodized aluminum conduit that extends through the building roof, which enables outdoor aerosol sampling from within the laboratory. BC concentrations in ambient air were much lower than in the flame exhaust. Samples were collected on quartz filters at an airflow rate of 3 L min^{-1} for 12–14 days per sample.

2.3. Pretreatment of quartz filters with salt

To investigate the catalytic influence of salts on the thermal regeneration of BC-laden filters, the filters were individually pretreated with four metal salts: NaCl, K_2CO_3, $CsNO_3$, and Cs_2CO_3. The filters were immersed in an aqueous salt solution (0.5 wt%) and then dried at 100 °C for 30 min inside a furnace. This dip-coating process likely resulted in a homogeneous distribution of discrete salt crystals on the fibers.

To determine the salt loading before and after BC collection and thermal regeneration, filters were soaked in 10 ml low-conductivity water and sonicated for 20 min to redissolve the salts. The resulting solutions were analyzed for anions (Cl^-, CO_3^{2-}, and NO_3^-) using a Dionex Ion Chromatography System (ICS, model 2000) and for cations (Na^+ and Cs^+) using a Dionex ICS DX-120. Calibration standards (0.1–10.0 mg L^{-1}) were prepared by diluting 1.000 g L^{-1} chromatography standards (Millipore Sigma). The calibration curves exhibited a relative standard deviation of 1.9% and a coefficient of determination (R^2) of 0.9998.

Molar ratios in this study represent the salt-to-carbon ratio. These were calculated by dividing the moles of the added salt by the moles of carbon in the BC sample, treating the BC as elemental carbon with a molecular weight of 12.0 g mol^{-1}. In the current study, the average molar loading ranged from 0.4–1.3 µmol cm^{-2} for $CsNO_3$ and Cs_2CO_3, and 2.3–3.9 µmol cm^{-2} for NaCl. Corresponding salt to BC molar ratios were 1.0–5.2 for $CsNO_3$ and Cs_2CO_3, and 5.6–15 for NaCl.

2.4. Thermal regeneration using a furnace

A temperature-programmable furnace (internal volume ~0.5 ft^3) was used to heat the quartz filters to target temperatures ranging from 475–670 °C at a rate of 40 °C min^{-1}. The furnace maintained the targeted temperatures for 5 min before turning off and enabled uniform heating of the filter with precise temperature control and reproducible regeneration conditions. Each filter underwent up to 10 cycles of aerosol collection and thermal regeneration to assess the durability of the catalytic effect.

2.5. Thermal regeneration using a prototype BC sensor

We fabricated a prototype sensor (Figure 1) that included (1) a filter holding platform with a central heating element that presses upward against the filter's back surface (Figure 2), (2) a retaining cover assembly featuring a glass window for visual inspection and lamp placement to enable optical transmission measurements, (3) a fiber-optic-positioned below the holding platform that transmits light to a spectrometer equipped with multi-channel array detection, and (4) an air inlet and outlet on opposite sides of the filter. The filter's perimeter is compressed between the retaining cover and platform using an O-ring and two clamps that ensured an airtight seal.

The prototype was capable of aerosol collection, thermal regeneration, and optical transmission measurement. During regeneration, a variable transformer controlled the voltage applied to the heating element while a K-type thermocouple beneath the filter monitored temperature. An inline power meter (HOBO UX120-018) recorded the applied voltage, current draw, and total energy consumption (power × time). Unlike the slow, uniform heating of the laboratory furnace, the sensor's heating element achieved rapid but non-uniform filter heating. Additionally, the location of the thermocouple tip was not precisely controlled. Thus, the required regeneration energy input—rather than measured temperature (which typically ranged between 470 and 600 °C)—served as a more meaningful parameter for evaluating the catalytic effects of salts.

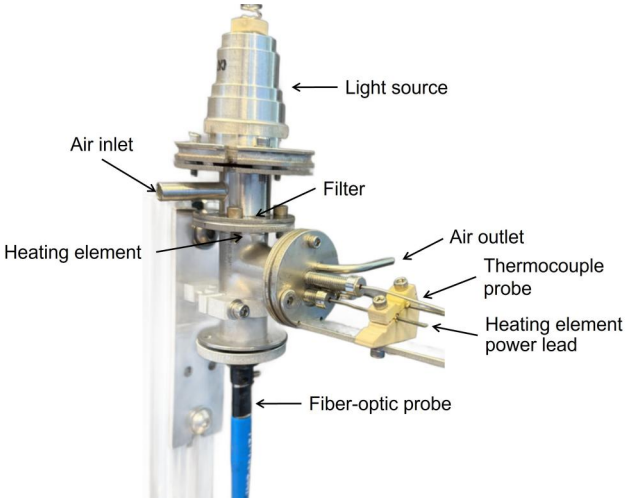

Figure 1. The prototype sensor capable of BC collection, thermal regeneration, and optical transmission measurement.

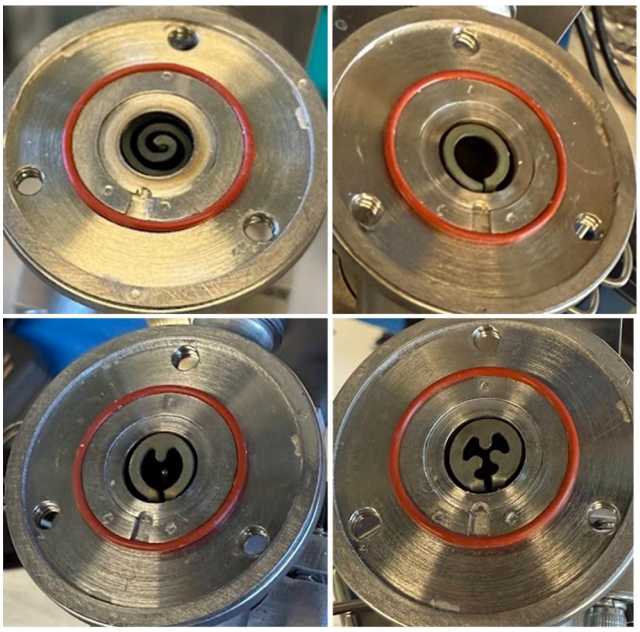

Figure 2. Photos of four heating elements used in the prototype sensor.

We evaluated four distinct nichrome heating element configurations: (1) spiral, (2) circular ring, (3) single-spike ring, and (4) three-spike ring (Figure 2). While the spiral configuration provided the largest heating surface area, it significantly blocked the optical path. The ring-shaped heaters were designed to minimize obstruction of the optical path between the light source and the fiber-optic probe aligned with the open center of the ring.

2.6. Optical transmission measurement

A custom-made optical spectrometer was used to measure the light transmitted through all filter samples before BC collection and after heating in both the furnace and the prototype sensor. The amount of BC on filters (μg cm^{-2}) was estimated as in Hansen et al. (1984):

$$BC = \frac{ATN}{\sigma}$$

where light attenuation (ATN) was calculated based on measured light intensities I_0 and I, which correspond to blank and BC-laden filters, respectively:

$$ATN = 100\ \ln\left({}^{I_o}/_{I}\right)$$

In filter-based aerosol optical absorption photometers, the wavelength-dependent attenuation coefficient (σ, $m^2\ g^{-1}$) is used to convert measured ATN to BC loading. In this study, we estimated BC loading from intensity measurements in the infrared (880 nm) assuming an attenuation coefficient of 16.6 $m^2\ g^{-1}$, which was derived partly from the work of Gundel et al. (1984). There is a rich body of literature showing σ may vary with aerosol-type and ATN diminishes with increasing BC loading (Hansen et al. 1984; Petzold et al. 2002; Weingartner et al. 2003; Collaud Coen et al. 2010; Drinovec et al. 2015; Titos et al. 2017). In this study demonstrating the thermal-regeneration mechanism and catalytic effect of salts, highly accurate BC loading measurements were not critical and, thus, these influences were not considered.

3. Results and discussion

3.1. Thermal regeneration using a furnace

Multiple filters were prepared with BC from the inverted methane flame, with initial transmission values (prior to heating) at 880 nm ranging from 0.44 to 0.60 (Figure 3). This corresponds to ATN_{880nm} values of 50 to 82 and BC loadings of 3.0 to 4.9 μg cm^{-2}. These amounts of BC are comparable to what would normally be collected when filter-based aerosol absorption photometers are used in ordinary environments. To evaluate regeneration efficiency, both unsalted and salted filter samples were heated in the furnace to at least two temperatures. As shown in Figure 3(a), transmission increased from an initial value of 0.6 before heating to 0.8 after heating to 640 °C, meaning that BC removal from unsalted filters was incomplete at 640 °C. Upon further heating to 665 °C, transmission increased to 1.0, corresponding to a clean white filter and complete BC removal. Much lower temperatures were required to regenerate the BC samples collected on salted filters: 500 °C for NaCl, $CsNO_3$, and K_2CO_3, and 475 °C for Cs_2CO_3, as

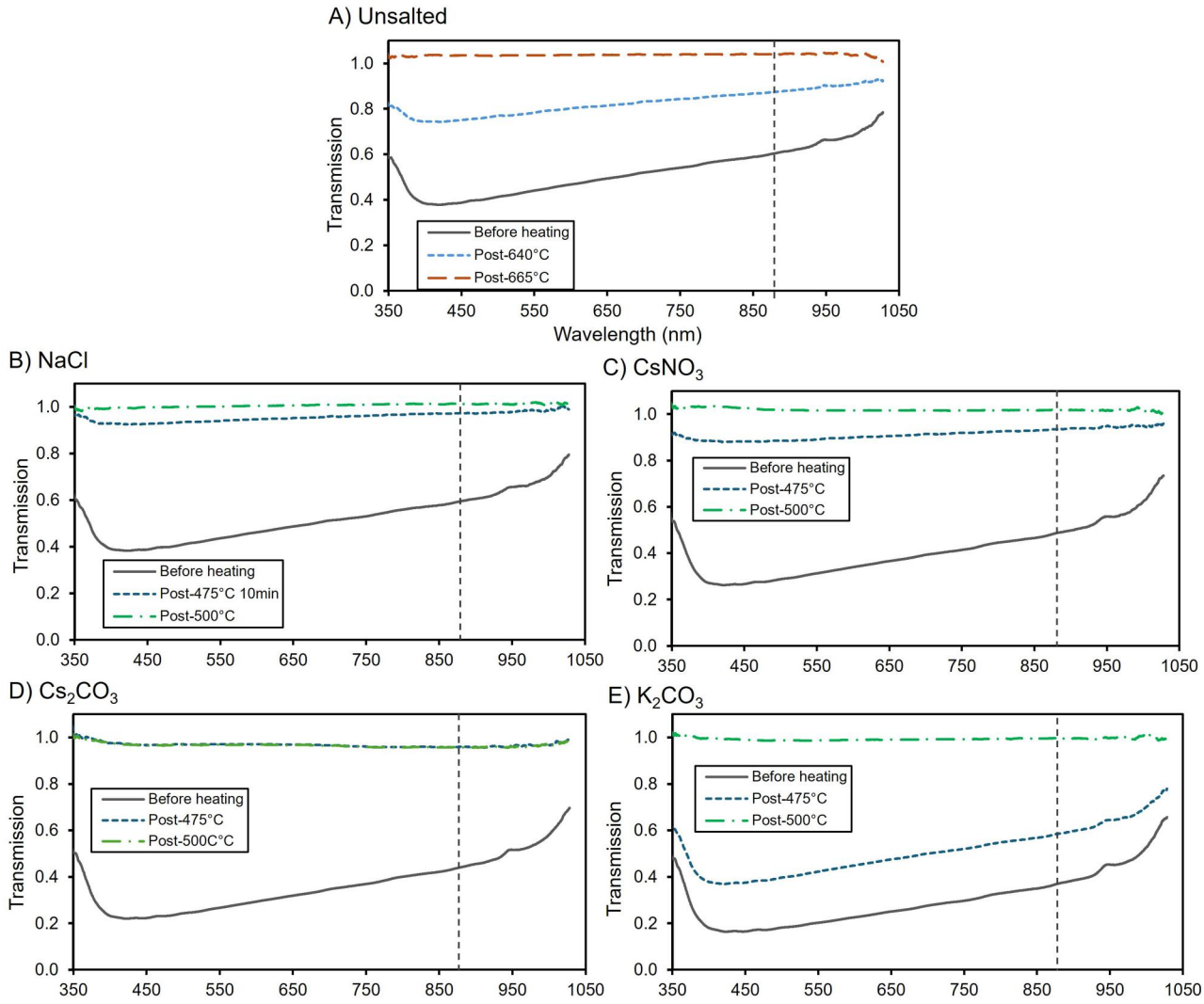

Figure 3. Optical transmission of laboratory flame BC-loaded filters before and after heating to different temperatures (indicated in figure legends) and holding for 5 min (10 min at 475°C in panel b). Before collecting flame-generated BC particles, filters were (a) unsalted or salted with water solutions of (b) NaCl, (c) $CsNO_3$, (d) Cs_2CO_3, and (e) K_2CO_3. The vertical dashed lines in each figure panel indicate the 880 nm wavelength.

shown in Figures 3b–e. The 165 °C temperature reduction observed for the NaCl sample is comparable to the 150 °C reduction reported by Kirchstetter and Novakov (2007), despite the very different approach used to apply salt to the filter. The lower regeneration temperature required for Cs_2CO_3–which corresponds to 190 °C reduction in regeneration temperature–demonstrates its superior catalytic activity for BC removal compared to NaCl, K_2CO_3, and $CsNO_3$.

Complete removal of ambient aerosol BC from unsalted quartz filters required heating to 700 °C (Figure 4a), higher than the 665 °C needed for flame-generated BC and likely due to the different chemical composition of the ambient and flame-generated aerosols. Filters impregnated with Cs_2CO_3 achieved full regeneration at 550 °C (Figure 4d), also a higher temperature than that required for complete removal of flame BC (475 °C). The 150 °C reduction in the temperature required for filter regeneration of ambient aerosol BC is lower than that for the flame BC (190 °C) but still indicative of the significant catalytic activity of Cs_2CO_3.

Notably, the filter center exhibited a persistent brown discoloration following thermal regeneration of ambient PM (Figure S1 in the online supplemental information [SI]), as corroborated by the residual transmission at wavelengths less than ~600 nm after heating (Figure 4b). We attribute this residual coloration to noncombustible inorganic constituents present in the ambient PM–likely iron oxides from soil dust–as there was building construction activity near

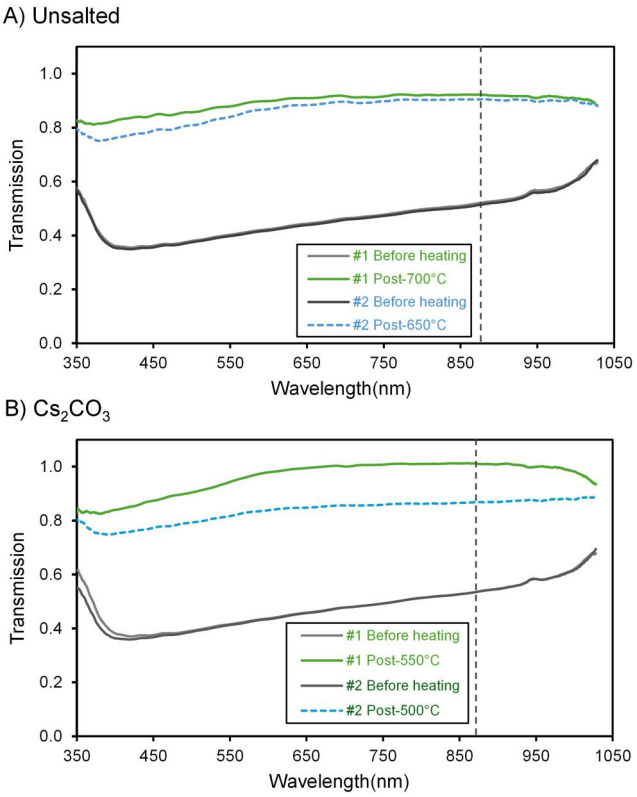

Figure 4. Transmission of filters loaded with ambient aerosol before and after heating to different temperatures in the furnace with a hold for 5 min. Before collecting ambient aerosol, the filters were (a) unsalted and (b) salted with solution of Cs_2CO_3. #1 and #2 denote distinct filter replicates used in each test. The vertical dashed lines in each figure panel indicate the 880 nm wavelength.

the aerosol sampling site and we did not use a size-selective inlet such as a cyclone to exclude coarse soil-derived particles during sample collection.

3.2. Thermal regeneration within the prototype sensor

The prototype sensor (Figure 1) was used with different filter heating elements (Figure 2) to evaluate thermal regeneration of flame BC and ambient aerosol BC on salted and unsalted filters. A constant 25–35 W power input was applied to the heating element until the measured optical transmission recovered to 1.0 ± 0.1, confirming complete BC removal from the filter. Heating duration varied significantly ($p < 0.05$) depending on the salt used, with Cs_2CO_3 enabling quickest regeneration (~50 s with single-spike ring heater), 11 times faster than unsalted filters (570 s), 7 times faster than NaCl (365 s), and 4 times faster than $CsNO_3$ (192 s). As shown in Figure 5 and Table S1, unsalted filters required 1.4–14 times more energy for

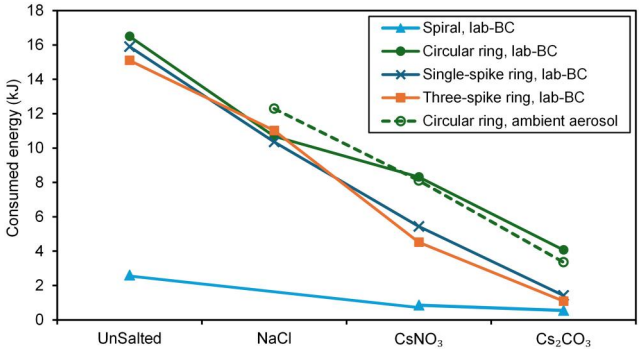

Figure 5. Energy (kJ) required to thermally regenerate unsalted and salted (NaCl, $CsNO_3$, and Cs_2CO_3) quartz filters in the prototype sensor using heating elements of various shapes (see Figure 2) following collection of flame-generated BC. Energy was calculated from measured voltage, current, and heating duration (see Table S1).

complete regeneration than salted filters, irrespective of heating element geometry. Cs_2CO_3-treated filters required the lowest energy input: one-tenth (three-spike ring-shaped heater) to one-quarter (circular ring-shaped heater) of the energy needed for regeneration of unsalted filters. This trend in energy savings associated with the various salts (Cs_2CO_3 > $CsNO_3$ > NaCl) follows the temperature reduction trends observed in the thermal regeneration tests using the furnace.

The performance differences between heater geometries were significant: the spiral shape required the least energy and the single- and three-spike shapes required less than the standard ring. These different energy input requirements are attributed to differences in the amount of direct thermal contact between the filter and the heater surface, which affect BC removal. For example, during thermal regeneration with the ring heater in the prototype sensor, BC was removed almost instantly from the filter perimeter in direct contact with the heating element, followed by progressive removal inward toward the filter center. Although the circular ring-shaped heater requires higher energy input to achieve filter regeneration, it provides the least obstructed optical path, which is desirable for increasing the amount of light incident on the fiber-optic probe.

Whereas higher furnace temperatures were required to remove ambient BC compared with laboratory flame-generated BC, regeneration energy inputs in the prototype sensor were similar for the two BC sources. For example, the energy required to regenerate $CsNO_3$-treated filters was 8.3 kJ for flame-generated BC and 8.1 kJ for ambient BC when the sensor was equipped with the circular ring-shaped heating element (Figure 5 and Table S1). These results indicate

that the choice of alkali metal salt and heating-element geometry exerts a greater influence on regeneration energy requirements than the BC source. This is not surprising, given that differences in regeneration temperatures are much more pronounced between samples collected on unsalted and salted filters than between flame-generated and ambient aerosol. For example, the regeneration temperature differences between unsalted and Cs_2CO_3-treated filters are 190 °C for flame-generated BC and 150 °C for ambient aerosol, whereas the corresponding differences between flame-generated and ambient BC are much smaller—35 °C for unsalted filters and 75 °C for Cs_2CO_3-treated filters.

3.3. Durability of the catalytic effect

The durability of the catalytic effect was evaluated by subjecting salted filters to 10 consecutive cycles of BC collection and thermal regeneration in both the prototype sensor and the laboratory furnace. To achieve complete regeneration in the prototype sensor, heating durations were tailored to the observed BC removal rates of each salt–2 min for Cs_2CO_3, 5 min for $CsNO_3$, and 7 min for NaCl–while maintaining a constant power supply of 25–28 W to the circular ring-shaped heating element. Under these conditions, the optical transmission at 880 nm of both Cs_2CO_3- and $CsNO_3$-treated filters consistently recovered to 1.00 ± 0.05 (Figure 6), demonstrating sustained catalytic activity. Consistent results were obtained in the furnace experiments, where heating to 500 °C for 5 min completely removed BC after every cycle (Figure 6); in contrast, as noted above, BC removal from unsalted filters was incomplete until heating to 665 °C. The sustained catalytic effect over repeated thermal cycling is consistent with previous studies (Peng et al. 2008; Skrbek et al. 2022).

As part of our assessment of the durability of the catalytic effect over repeated cycles of heating, filters were sonicated in water to redissolve the salts (as described in Section 2.3). Interestingly, ion chromatography results indicated substantial loss of water-soluble salts. As shown in Figure S2A, the apparent retention of water-soluble salts on filters heated in the furnace followed the order of their melting points: NaCl (83–98%, 801 °C) > Cs_2CO_3 (37–44%, 610 °C) > $CsNO_3$ (2–3%, 414 °C). The calculated losses of $CsNO_3$ and Cs_2CO_3 are likely related to their thermal decomposition (Stern 1972; Yanase et al. 2006), which alters their molecular form, or to chemical reactions that bind cesium to the quartz fibers (Glenn et al. 2019). In either case, this would explain why the cesium becomes unrecoverable by the aqueous extraction while its catalytic effect persists over multiple heating cycles. The higher retention of NaCl likely reflects its extreme resistance to thermal decomposition. The significantly higher recovery of the water-soluble salts from filters heated in the prototype sensor (>70%; Figure S2B) is likely due to differences in heating profiles: filters are heated slowly and uniformly in the furnace, whereas heating in the sensor is rapid and non-uniform, with regions in direct contact with the heating element reaching higher temperatures than portions heated indirectly. The shorter heating duration, combined with cooler temperatures across portions of the filter, may limit thermal decomposition of the salts.

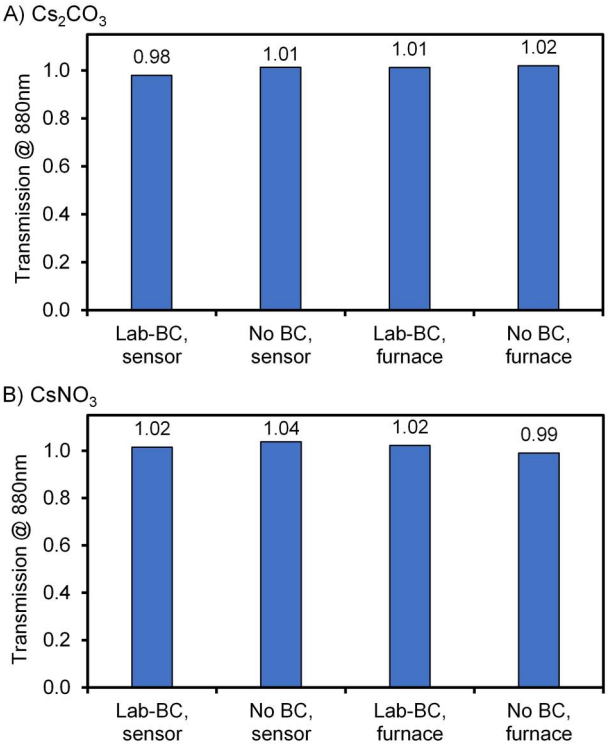

Figure 6. Optical transmission at 880 nm following 10 cycles of thermal regeneration in the prototype sensor and furnace. Transmission is shown for filters treated with (a) Cs_2CO_3 and (b) $CsNO_3$. In each cycle, BC was collected on the filter prior to thermal regeneration; regeneration without BC collection served as control.

4. Conclusions

Based on the results of the current study, an energy-efficient and reduced maintenance BC sensor is achievable and warrants further development. The demonstrated reduction in filter regeneration temperature provided by pretreatment with metal salts,

especially Cs_2CO_3 (190 °C for flame-generated BC and 150 °C for ambient BC), offers practical benefits for a BC sensor, including lower energy requirements for filter regeneration. For example, we estimate using Cs_2CO_3-treated filters would enable 4–14 times more thermal regeneration cycles than untreated filters under battery-powered operation due to the reduced energy requirement. Lower thermal regeneration temperature and duration also means reduced thermal stress on sensor components and improved long-term device reliability.

Ambient aerosol sampling introduced some complexities including the accumulation of noncombustible material and filter discoloration, which can increase airflow resistance and interfere with the optical measurements of BC concentration. However, these effects can be accounted for algorithmically in post-processing. Future work will focus on transitioning the benchtop prototype sensor to a field-deployable sensor and evaluating its performance across diverse ambient environments.

Disclosure statement

F. J. Brechtel is affiliated with Brechtel Manufacturing Inc., which develops and sells black carbon measurement instruments.

Funding

This research was funded by California Air Resources Board under agreement number 21MLD035. The Lawrence Berkeley National Laboratory operates under the U.S. Department of Energy contract No. DE-AC02-05CH11231.

References

Airvisual pro indoor monitor. n.d. IQ Air. https://www.iqair.com/us/products/air-quality-monitors/airvisual-pro-indoor-monitor?Title=Default+Title

Caubel JJ, Cados TE, Kirchstetter TW. 2018. A new black carbon sensor for dense air quality monitoring networks. Sensors. 18(3):738. doi. https://doi.org/10.3390/s18030738

Caubel JJ, Cados TE, Preble CV, Kirchstetter TW. 2019. A distributed network of 100 black carbon sensors for 100 days of air quality monitoring in West Oakland, California. Environ Sci Technol. 53(13):7564–7573. https://doi.org/10.1021/acs.est.9b00282

Chen SG, Yang RT. 1992. Mechanism of alkali and alkaline earth catalyzed gasification of graphite by co2 and h2o studied by electron microscopy. J Catal. 138(1):12–23. https://doi.org/10.1016/0021-9517(92)90003-Z

Clarity node-s air sensor. n.d. Clarity movement Co. https://www.clarity.io/products/clarity-node-s?utm_term=air%20quality%20monitor&utm_campaign=Leads-Search-Q3-2022+%5BClicks%5D&utm_source=adwords&utm_medium=ppc&hsa_acc=1787529554&hsa_cam=21990037659&hsa_grp=172761752058&hsa_ad=724573365316&hsa_src=g&hsa_tgt=kwd-16767816&hsa_kw=air%20quality%20monitor&hsa_mt=b&hsa_net=adwords&hsa_ver=3&gad_source=1&gad_campaignid=21990037659&gbraid=0AAAAACPUJUMqMYTu7NJYJpCATiHeTSNLR&gclid=Cj0KCQjwjdTCBhCLARIsAEu8bpIbFFssQP7A2var-BY5MqdFrpdMjx_fUZCWSzULyG3jb0GtEM_tnIoaAr_wEALw_wcB

Collaud Coen M et al. 2010. Minimizing light absorption measurement artifacts of the aethalometer: evaluation of five correction algorithms. Atmos Meas Tech. 3(2):457–474. https://doi.org/10.5194/amt-3-457-2010

Drinovec L et al. 2015. The "dual-spot" aethalometer: an improved measurement of aerosol black carbon with real-time loading compensation. Atmos Meas Tech. 8(5):1965–1979. https://doi.org/10.5194/amt-8-1965-2015

Glenn M, Allen JA, Donne SW. 2019. Silicate formation in a ternary alkali metal carbonate melt. Energy Fuels. 33(11):12008–12015. https://doi.org/10.1021/acs.energyfuels.9b02356

Gundel LA, Dod RL, Rosen H, Novakov T. 1984. The relationship between optical attenuation and black carbon concentration for ambient and source particles. Sci Total Environ. 36:197–202. https://doi.org/10.1016/0048-9697(84)90266-3

Hansen ADA, Rosen H, Novakov T. 1984. The aethalometer—an instrument for the real-time measurement of optical absorption by aerosol particles. Sci Total Environ. 36:191–196. https://doi.org/10.1016/0048-9697(84)90265-1

Heintzelman A et al. 2023. Efficacy of low-cost sensor networks at detecting fine-scale variations in particulate matter in urban environments. Int J Environ Res Public Health. 20(3):1934. https://doi.org/10.3390/ijerph20031934

Jiménez R, García X, López T, Gordon AL. 2008. Catalytic combustion of soot. Effects of added alkali metals on cao-mgo physical mixtures. Fuel Process Technol. 89(11):1160–1168. https://doi.org/10.1016/j.fuproc.2008.05.013

Kapteijn F, Peer O, Moulijn JA. 1986. Kinetics of the alkali carbonate catalysed gasification of carbon: 1. Co2 gasification. Fuel. 65(10):1371–1376. https://doi.org/10.1016/0016-2361(86)90107-9

Karagulian F et al. 2019. Review of the performance of low-cost sensors for air quality monitoring. Atmosphere (Basel). 10(9):506. https://doi.org/10.3390/atmos10090506

Kirchstetter TW, Novakov T. 2007. Controlled generation of black carbon particles from a diffusion flame and applications in evaluating black carbon measurement methods. Atmos Environ. 41(9):1874–1888. https://doi.org/10.1016/j.atmosenv.2006.10.067

Kumar P et al. 2015. The rise of low-cost sensing for managing air pollution in cities. Environ Int. 75:199–205. https://doi.org/10.1016/j.envint.2014.11.019

Lassalle MW. 2024. The present state of low-cost air quality sensors in japan and their accuracy. Int J Environ Stud. 81(4):1665–1683. https://doi.org/10.1080/00207233.2024.2358716

Legutko P et al. 2023. Catalytic soot combustion-general concepts and alkali promotion. ACS Catal. 13(5):3395–3418. https://doi.org/10.1021/acscatal.2c05994

Lewis AC et al. 2016. Evaluating the performance of low cost chemical sensors for air pollution research. Faraday Discuss. 189:85–103. https://doi.org/10.1039/C5FD00201J

Liu X et al. 2020. Low-cost sensors as an alternative for long-term air quality monitoring. Environ Res. 185: 109438. https://doi.org/10.1016/j.envres.2020.109438

McKee DW. 1983. Mechanisms of the alkali metal catalysed gasification of carbon. Fuel. 62(2):170–175. https://doi.org/10.1016/0016-2361(83)90192-8

Mochida I, Miyazaki T. 1998. Reactivities of several carbonaceous materials for their combustion catalyzed by potassium salts on perovskite type oxide. Energy Fuels. 12(5): 939–944. https://doi.org/10.1021/ef980019b

Morawska L et al. 2018. Applications of low-cost sensing technologies for air quality monitoring and exposure assessment: how far have they gone? Environ Int. 116: 286–299. https://doi.org/10.1016/j.envint.2018.04.018

Neeft JPA, Makkee M, Moulijn JA. 1998. Catalytic oxidation of carbon black - i. Activity of catalysts and classification of oxidation profiles. Fuel. 77(3):111–119. https://doi.org/10.1016/S0016-2361(97)00187-7

Peng Q, Wei X, Ding J, Yang J, Yang X. 2008. High-temperature thermal stability of molten salt materials. Int J Energy Res. 32(12):1164–1174. https://doi.org/10.1002/er.1453

Petzold A, Kramer H, Schönlinner M. 2002. Continuous measurement of atmospheric black carbon using a multi-angle absorption photometer. Environ Sci Pollut Res Special Issue. 4:78–82.

Skrbek K, Bartůněk V, Sedmidubský D. 2022. Molten salt-based nanocomposites for thermal energy storage: materials, preparation techniques and properties. Renew Sustain Energy Rev. 164:112548. https://doi.org/10.1016/j.rser.2022.112548

Stavroulas I et al. 2020. Field evaluation of low-cost pm sensors (purple air pa-ii) under variable urban air quality conditions, in greece. Atmosphere (Basel). 11(9):926. doi. https://doi.org/10.3390/atmos11090926

Stern KH. 1972. High temperature properties and decomposition of inorganic salts part 3, nitrates and nitrites. J Phys Chem Refer Data. 1(3):747–772. https://doi.org/10.1063/1.3253104

Stipe CB, Higgins BS, Lucas D, Koshland CP, Sawyer RF. 2005. Inverted co-flow diffusion flame for producing soot. Rev Scient Instrum. 76(2):023908. https://doi.org/10.1063/1.1851492

Sugrue RA et al. 2024. The value of adding black carbon to community monitoring of particulate matter. Atmos Environ. 325:120434. https://doi.org/10.1016/j.atmosenv.2024.120434

Suzuki T, Ohme H, Watanabe Y. 1992. Alkali metal catalyzed carbon dioxide gasification of carbon. Energy Fuels. 6(4):343–351. https://doi.org/10.1021/ef00034a003

Titos G et al. 2017. Spatial and temporal variability of carbonaceous aerosols: assessing the impact of biomass burning in the urban environment. Sci Total Environ. 578:613–625. https://doi.org/10.1016/j.scitotenv.2016.11.007

Weingartner E et al. 2003. Absorption of light by soot particles: determination of the absorption coefficient by means of aethalometers. J Aerosol Sci. 34(10):1445–1463. https://doi.org/10.1016/S0021-8502(03)00359-8

Yanase I, Konakawa J, Kobayashi H. 2006. Influence of cesium nitrate and heating rate on densification and microstructure of cs-deficient pollucite sintered body. J Amer Ceram Soc. 89(1):184–188. https://doi.org/10.1111/j.1551-2916.2005.00703.x